Analysis of a DVR with Molten Carbonate Fuel Cell and Fuzzy Logic Control

Jaydeep Chakravorty
Electrical Engineering Department
Indus University
Ahmedabad, India

Geena Sharma
Electrical Engineering Department
Baddi University
Himachal Pradesh, India

Vinay Bhatia
Electrical & Electronics Engineering
Department, Baddi University
Himachal Pradesh India

***Abstract*—As power demand constantly (and rapidly) increases and with the introduction of many sophisticated electronic devices, power quality issues are becoming a major problem for the power sector. In this context, issues of power quality, voltage swells and sags have become rather common. Custom power devices are generally used to solve this problem. A dynamic voltage restorer (DVR) is the most efficient and effective modern custom power device used in power distribution networks. In this paper a new DVR model is presented. The proposed DVR has a molten carbonate fuel cell (MCFC) as its DC source of supply with an ultra-capacitor along with a fuzzy controller as its controlling unit. The complete model is implemented in MATLAB/SIMULINK and the output of the proposed model is compared with conventional DVR model with a simple DC voltage source and a capacitor with the same fuzzy controller**

Keywords-DPFC; MCFC; ultra capacitor; fuzzy logic

I. INTRODUCTION

As the complexity of power systems increases, voltage swells and sags are becoming common issues. A dynamic voltage restorer (DVR) is considered an economical and very effective device to improve the voltage swell and sag in the system [1, 2]. DVRs are a class of custom power devices for providing reliable distribution power quality. They employ a series of voltage boost technology using solid state switches for compensating voltage sags/swells. DVRs are mainly used to protect for sensitive loads that may be drastically affected by fluctuations in system voltage. A DVR gives good result when used in the case of low or medium voltage distribution [3, 4]. Other than voltage sags and swells compensation, a DVR can also add other features like: line voltage harmonics compensation, reduction of transients in voltage and fault current limitations. In this paper a new DVR model implemented in MATALB/SIMULINK is presented. The proposed DVR employs a molten carbonate fuel cell (MCFC) as its DC source of supply with an ultra-capacitor along with a fuzzy controller as its controlling unit. The model's behavior is investigated and compared to a more conventional DVR model.

II. MOLTEN CARBONATE FUEL CELL

The schematic model of a Molten Carbonate Fuel Cell (MCFC) is shown in Figure 1. A fuel cell converts chemical energy into electrical energy. In the MCFC, the CO_2 gas moves from cathode to anode through a molten electrolyte. Here molten carbonate salt acts as an electrolyte where two porous electrodes are present. The electrode layer is formed in sub layers. Between the gas and the electrode a thin porous metal plate is inserted acting as a diffuser, it helps in helping the gas mixture to enter the porous electrode. When the CO_2 combines with O_2 in the cathode gives carbonate ions and when it combines with hydrogen in the anode side it gives CO_2 and H_2O. So there will be a movement of electrolyte from anode side to the cathode side. The gas reaction at the anode side is

$$CO + H_2O \leftrightarrow CO_2 + H_2 \quad (1)$$

The electrochemical half reaction is

$$H_2 + CO_3^{--} \leftrightarrow CO_2 + H_2O + 2e \quad (2)$$

Similarly the equation of cathode side will be

$$\frac{1}{2}O_2 + CO_2 + 2e \leftrightarrow CO_3^{--} \quad (3)$$

The equivalent electrical circuit of a singular cell MCFC is shown in Figure 2 [5], where, R_i is the ionic resistance, R_e is the electronic resistance and R_{load} is the external load resistance. Electrically, a single cell acts as the parallel of elementary real generators, each of which is a fraction of the cell thickness from anode to the cathode. If the fuel cell is having generic (N, k) strip, where, N=1,2,……. N_{chA} and k=1,2,……..N_{chc}) then the total current flow and also the potential difference is given by:

$$i_{load} = \sum_{N=1,k=1}^{Ncha,Nchc} i_{N,k} \quad (4)$$

$$V_{out} = E - i_{N.k} \times R_{load} = i_{load} \times R_{load} \quad (5)$$

where, E is the Nernst voltage of (N,k) strip, and is given by:

$$E = E_0 + \frac{RT}{2F} ln\left(\frac{P_{H_2}P_{02}^{0.5}}{P_{H2O}} \times P_{CO2}\right) \quad (6)$$

where, E_0 is the standard condition potential and the neutral component concentrations refer to the gas diffused into the liquid electrolyte. Single cell voltage is given by (7) [5]:

$$V_c = \frac{E_m - \eta_f \times i_m \times R_i}{\frac{R_i}{R_e} \times (1-\eta_f)+1} = E_r - i(\mu_a + \mu_c + \mu_o) \quad (7)$$

where, E_r is the reversible voltage of the cell, μ_α the activation voltage, $\mu_c=-V_{CO}$ the concentration voltage, $\mu_0=-V_0$ the ohmic voltage.

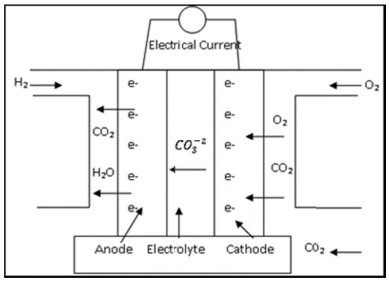

Fig. 1. Molten carbonate fuel cell.

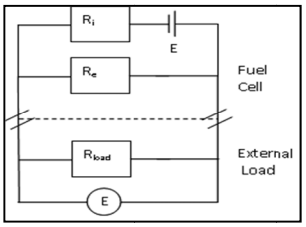

Fig. 2. Electrical equivalent of MCFC.

Again,

$$E_r = 1.2 - 9\times10^{-4}(T-298) + T4.3\times10^{-5}\left(\ln P_{H_2} + \frac{1}{2}\ln P_{CO_2}\right) \quad (8)$$

$\mu_a = 2.3\times10^{-10}\times P_{H2}\times P_{CO2}\times P_{H2o}\times e^{\left(\frac{E}{RT}\right)}$ is the activation polarization losses, $\mu_c = 7.5\times10^{-10}\times P_{o2}\times P_{co2}\times e^{\left(\frac{E}{RT}\right)}$ the concentration polarization losses and $\mu_0 = 0.45\times10^{-5}e^{\left(8600\times\left(\frac{1}{T}-\frac{1}{925}\right)\right)}$ the ohmic polarization loss. where,

$$P_{H2} = 0.5P_{H2O}\left(exp\left(-\frac{1.635J}{T^{1.334}}\right)\frac{P_a}{P_{H2O}} - 1\right) \quad (9)$$

$$P_{O2} = P_{H2O}\left(exp\left(-\frac{4.192J}{T^{1.334}}\right)\frac{P_c}{P_{H2O}} - 1\right) \quad (10)$$

$$P_{CO_2} = \frac{P_{O_2}}{5.08\times10^6\times e^{-498/T}} \quad (11)$$

$$\log P_{H_2O} = -2.18 + 2.95\times10^{-2}T_C - 9.18\times10^{-5}T_C^2 + 1.44\times10^{-7}T_C^3$$

where, $T_c=T-274$. The thermal capacitance for all the volume or mass of the fuel=10J/K is expressed by (12):

$$Ct\frac{dT}{dt} = i(E_r - V_c) - H(T - T_f) \quad (12)$$

where, H is the total heat transfer coefficient (10W/K), T_f the reference temperature (300K), P_a the partial pressure for anode (1.5), P_c the partial pressure for cathode (1) and J the current density (1). The kinetic equation of the chemical reaction in MCFC is tabulated in Table I. The physical properties and the operating conditions are tabulated in Tables II and III respectively. The complete detail of the mathematical model is tabulated in Table IV.

TABLE I. CHEMICAL REACTION WITH KINETIC EQUATION

Chemical Reactions	Kinetic Equation
$CH_4 + H_2O \rightarrow CO + 3H_2$	$R_1 = \frac{\frac{K_1}{P_{H2}^{2.5}}\left(P_{CH_4}P_{H_2o} - \frac{P_{H2}^3 P_{CO}}{K_{eq1}}\right)}{D^2}$
$CO + H_2O \rightarrow H_2 + CO_2$	$R_2 = \frac{\frac{K_2}{P_{H_2}}\left(P_{CO}P_{H_2o} - \frac{P_{CO}P_{H_2}}{K_{eq2}}\right)}{D^2}$
$CH_4 + 2H_2O \rightarrow CO_2 + 4H_2$	$R_3 = \frac{\frac{K_3}{P_{H2}^{3.5}}\left(P_{CH_4}P_{H_2o}^2 - \frac{P_{H2}^4 P_{CO2}}{K_{eq3}}\right)}{D^2}$
$K_i = K_{iTr}e^{\left(\frac{-E_i}{R}\times\left(\frac{1}{T}-\frac{1}{Tr}\right)\right)}$	$K_j = K_{jTr}e^{\left(\frac{-\Delta h_j}{R}\times\left(\frac{1}{T}-\frac{1}{Tr}\right)\right)}$

TABLE II. PHYSICAL PROPERTIES

Property	Cathode	Anode	Electrolyte	Separator
Density (Kg/m^3)	6000	8000	2000	8100
Heat capacity ($J.Kg^{-1}K^{-1}$)	43000	390	4890	520
Heat Conduction ($W.m^{-1}.K^{-1}$)	3	30	30	30

TABLE III. CONDITIONS

Simulated Parameters	Values
Operating pressure	1 bar
Thickness (Cell)	1 cm
Thickness (Electrode)	1 mm
Thickness (Electrolyte)	1 mm
Area	1 m x 1m
Convection coefficient (Anode)	84 Wm-2K-1
Convection coefficient (Cathode)	90 Wm-2K-1
Activation energy (Anode)	50000 Jmol-1K-1
Activation energy (Cathode)	70000 Jmol-1K-1
Heat capacity (Anode)	4R
Heat capacity (Cathode)	4R

TABLE IV. MATHEMATICAL MODEL OF MCFC

Domain	Boundary
$C\left(\frac{\delta x_A}{\delta t} + V_x\frac{\delta x_A}{\delta x}\right) = \frac{1}{V_{ch}}\sum_j(R_{Aj} - x_A\sum_{\beta=1}^{N}R_{\beta j})$	$x_A(x=0,t) = x_{A0}$ $x_A(x,t=0) = x_{Ai}$
$CC_p\left(\frac{\delta T_{ac}}{\delta T} + V_s\frac{\delta T_{ac}}{\delta x}\right) =$ $\frac{q_{ac}}{V_{ch}} - \frac{1}{V_{ch}}\sum R_j\Delta h_j$ $q_T = q_{ac} + \sum R_j\Delta h_j \quad q_c$ $= Ah_c(T_s - T_c)$ $q_a = Ah_{as}(T_s - T_a)$ $n_sC_{ps}\frac{\delta T_s}{\delta t} = K_s\left(\frac{\delta^2 T_s}{\delta x^2}\right)$ $-\frac{R_{elec}\Delta h_{elect} - iV_{cea}}{V_s}$ $-\frac{A(h_{as}\times(T_s - T_a) + h_{cs}\times(T_s - T_a))}{V_s}$	$T_{ac}(x=0,t)$ $= T_{ac,0}$ $T_{ac}(x,t=0)$ $= T_{aci}$ $\frac{\delta T_s}{\delta x} = (x=0,t)$ $= 0$ $\frac{\delta T_s}{\delta x} = (x=L,t)$ $= 0$ $T_s(x,t=0) = T_{s,i}$

The equations are integrated along the anodic and cathodic x coordinate. Equations regarding catalytic medium are integrated along the z coordinate. [6]. ODEs are thus obtained from PDEs. This conversion decreases the complexity of the equations but on the other hand the volume of the equations increases. The ODEs are time discretized to obtain the approximate equations. These equations are then solved using iterative techniques. Thus the obtained ODEs are then simulated in MATLAB. For solving these equations, the ode23s MATLAB solver was selected. The SIMULINK model of various parts of MCFC is shown in Figures 3-8.

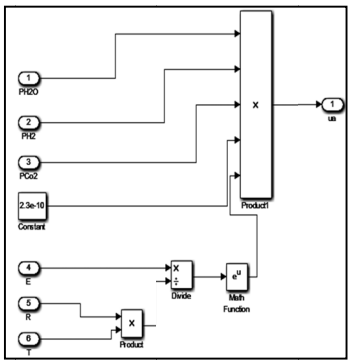

Fig. 3. Ohmic polarization loss model

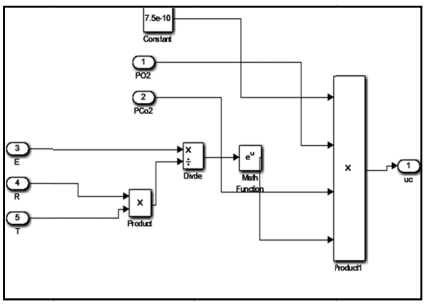

Fig. 4. Concentration polarizatio loss model.

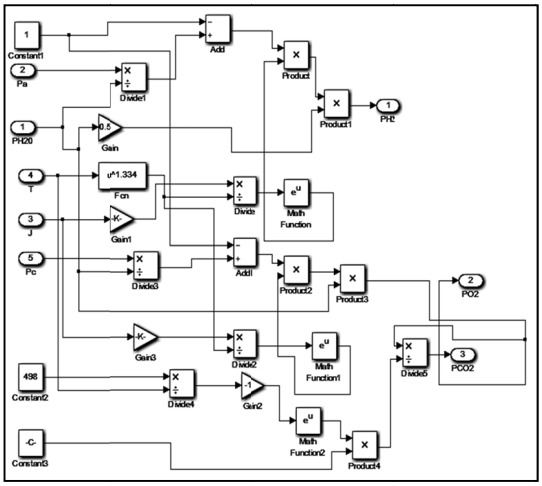

Fig. 5. Ohmic polarization loss model

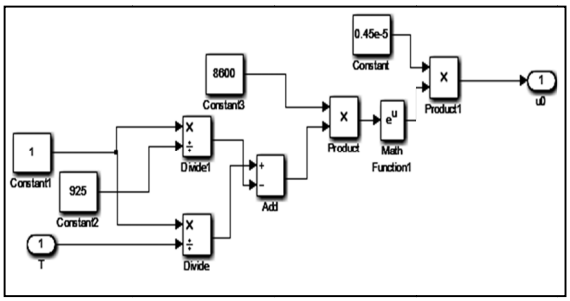

Fig. 6. PH_2, PO_2, PCO_2 model

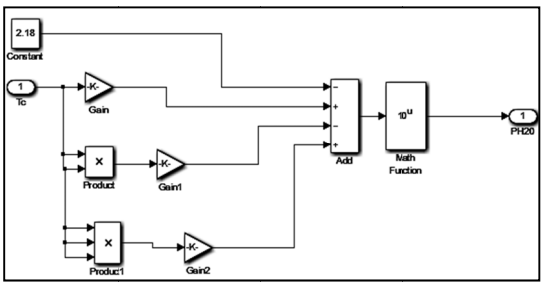

Fig. 7. PH_2O model

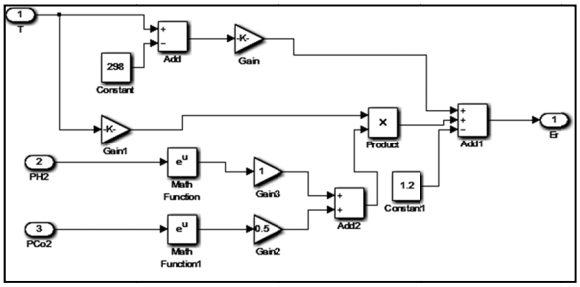

Fig. 8. Reversible voltage model

III. ULTRA CAPACITOR

Capacitor is a device used to store the charge in an electric circuit. An ultra-capacitor, also known as super capacitor is an electrical component capable of holding hundreds of times more electrical charge quantity than a standard capacitor. Unlike batteries, no chemical reaction takes place when energy is being stored or discharged and therefore an ultra capacitor can go through thousands of charging cycles with no degradation. Energy is stored in it by polarizing the electrolytic solution. The charges are separated via electrode-electrolyte interface. Ultra capacitor consists of a porous electrode, electrolyte and a current collector (metal plates). There are two carbon sheets separated by separator. The highly porous carbon can store more energy than any other electrolytic capacitor. When the voltage is applied to the negative plate, it attracts the positive ions from the electrolyte and when the voltage is applied to the positive plate, it attracts the negative ions from the electrolyte. Therefore there is a formation of a layer of ions on both plate sides and hence it is also called double layer capacitor. Capacitors are complementary to batteries as they deliver high power density and low energy density. The super

capacitor is a solution where ambient temperatures make it difficult to keep batteries inside the recommended operating range without compromising their capacity and lifetime. Super capacitor has high power and energy density, and therefore much higher efficiency. Conventional capacitors use dielectrics to increase capacitance by allowing plates to get very close. However practical problems on plate surface area and distance between plates reduce capacity. This drawback is overcomed by a super capacitor which provides large surface area with distance. Authors in [8] designed super capacitor based storage systems for elevator applications. The comparison between a battery and a super-capacitor is broken down in Table V.

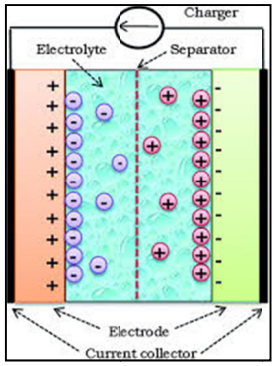

Fig. 9. Ultra capacitor

TABLE V. BATTERY – SUPER CAPACITOR COMPARISON

Features	Battery	Super capacitor
Power Range	Up to megawatts	Up to tens of thousands of kilowatts
Reliability	Moderate	High
Recharge time	10x discharge time	Seconds
Number of discharge cycles	Up to 3000	Up to 1 million
Operating Conditions	Narrow temperature range	Wide temperature range

IV. FUZZY CONTROLLER

In DVR the PI controller is the most common controller of the proper DVR operation. But efficiency of the PI controller decreases with an increase in the DVR range of operation. Nowadays, Fuzzy logic is being used in DVR control. This increases the efficiency and the reliability of the system to a greater extent. The fuzzy rules used are shown in Table VI. The phase of the voltage of the network is determined using a phase lock loop (PLL). After determination of the phase a reference signal of unity is generated to supply frequency for each phase of the system. The difference between reference signal of PLL and the actual supply voltage gives the error signal. So, the two inputs for the fuzzy controller are the error and the error rate. The output of the fuzzy controller when passing through PWM gives the pulse.

V. PROPOSED MODEL

The single line diagram of the system under test is shown in Figure 10. From the source, two parallel feeders are taken out. One of the feeders is connected with the DVR under test and the other feeder is not. The DVR has three operating modes, protection mode, standby mode and boost mode [9]. The DVR model has a source and a storage unit, a capacitor, inverter circuit and a filter circuit. In the proposed model, the MCFC has been used as a source for DVR along with ultra capacitor. The inverter circuit has IGBT in it and the filter circuit is an LC filter. The main function of the filter circuit is to keep the harmonic voltage generated by the power electronic devices present in the DVR to an acceptable value. The system parameters used for testing are given in Table VII. Two systems have been designed. First, the DVR model with simple DC source and a capacitor with fuzzy controller. The other, is the proposed DVR with MCFC as a source of supply and with ultra capacitor. The controller in both the system is kept the same.

TABLE VI. FUZZY RILES

e/Δe	PL	PM	PS	Z	NL	NM	NS
PL	PL	PL	PL	PM	PM	PS	Z
PM	PL	PL	PM	PM	PS	Z	NS
PS	PL	PM	PM	PS	Z	NS	NM
Z	PL	PL	PS	Z	NS	NM	NM
NL	PM	PS	Z	NS	NM	NM	NM
NM	PS	Z	NS	NM	NM	NM	NM
NS	Z	NS	NM	NM	NL	NL	NL

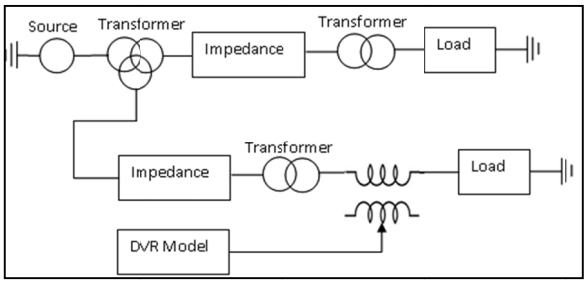

Fig. 10. Block diagram of test system

TABLE VII. TESTING PARAMETERS

Parameter	Value
Source	11KV, 50Hz, 3 Phase
Inverter	IGBT, 6 pulse, 3 arm, carrier frequency=1080Hz, Time 4μsec.
Load	Active power of 1KW, Reactive power of 500VAR
Two winding transformer	11KV/415V
Three winding transformer	11KV/415V/415V

VI. PROPOSED SIMULINK MODEL

The complete SIMULINK model of the MCFC after combining all the subsystems discussed above is shown in Figure 11. The models of ultra capacitor, fuzzy controller, complete DVR with simple voltage source and the proposed model of DVR with MCFC and ultra-capacitor are shown Figure 12, 13, 14 and 15 respectively.

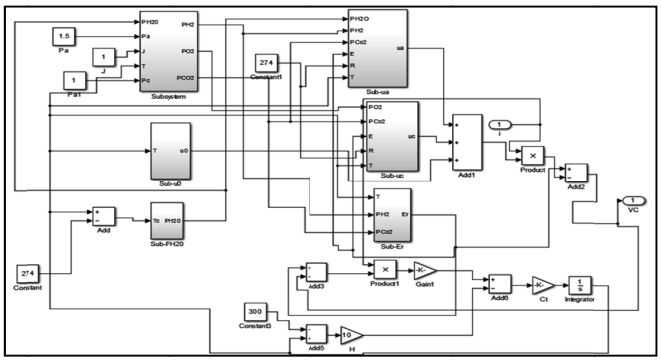

Fig. 11. MCFC SIMULINK model

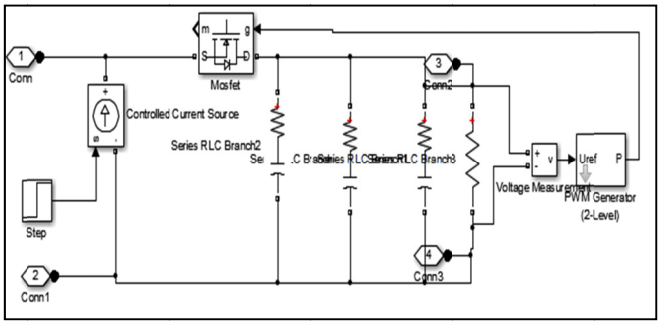

Fig. 12. Ultra capacitor SIMULINK model

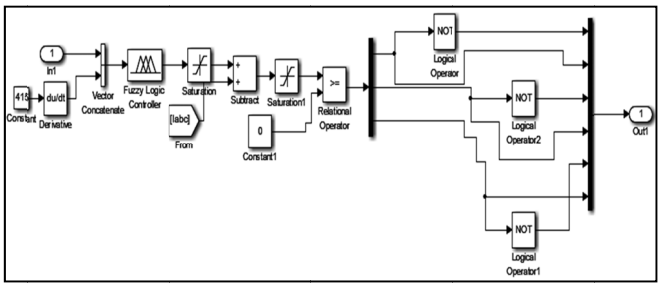

Fig. 13. Fuzzy controller SIMULINK model

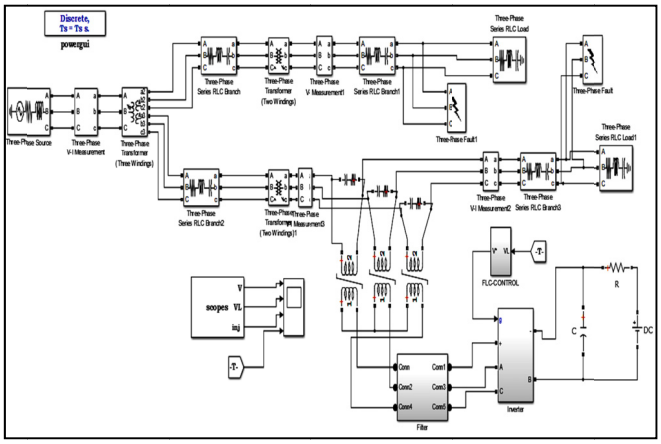

Fig. 14. DVR with sinple voltage source and capacitor SIMULINK model.

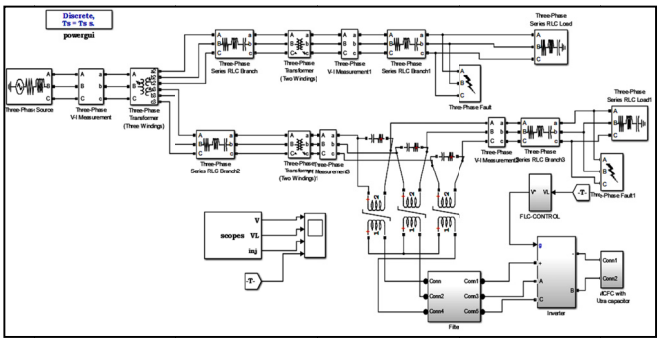

Fig. 15. DVR with MCFC and ultra capacitor.

VII. SIMULATED RESULTS

Before using the MCFC model in our proposed DVR, the behavior of the MCFC was compared with the experimental data available in the literature [7]. Results are shown in Figure 16. The behavior of the circuit, without DVR and with DVR (conventional model, Figure 14), for different fault conditions is described in Figures 17 to 25. The corresponding output waveform of the proposed DVR model with MCFC and ultra-capacitor for different fault conditions is shown in Figures 26 to 28. The comparative table for the two models is given in Table VIII.

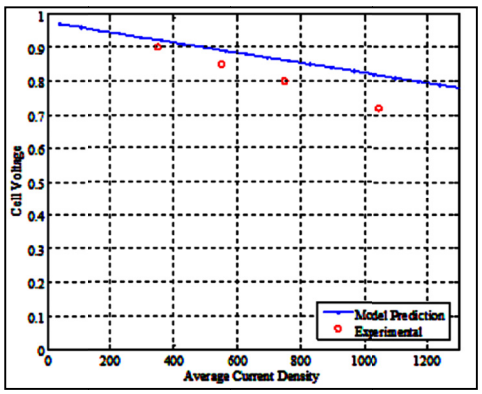

Fig. 16. Comparative graph

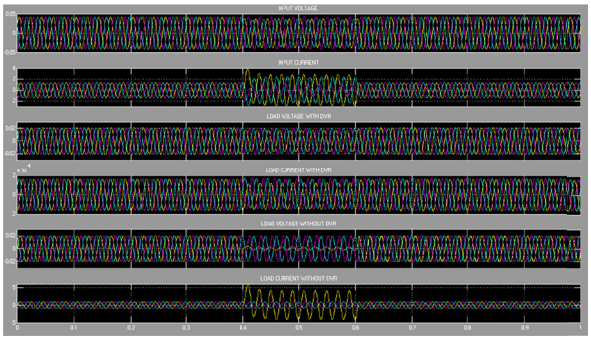

Fig. 17. Single line to ground fault.

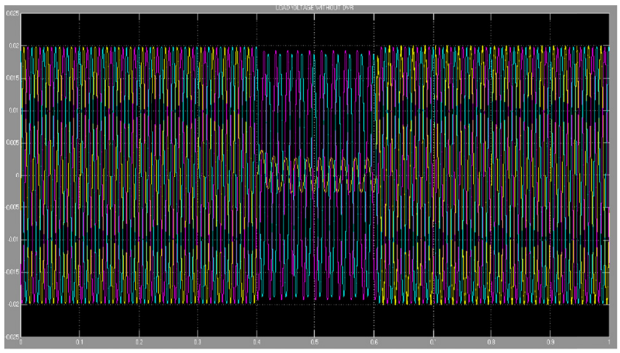

Fig. 18. Load votage without DVR

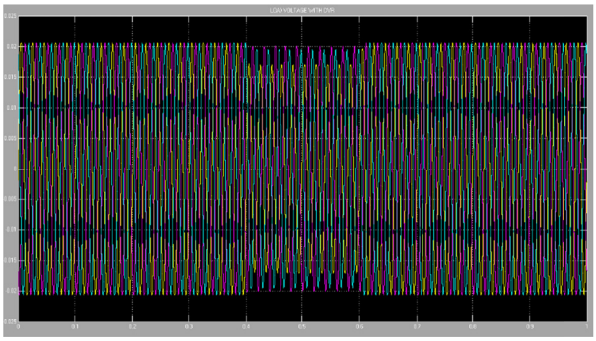

Fig. 19. Load voltage with DVR

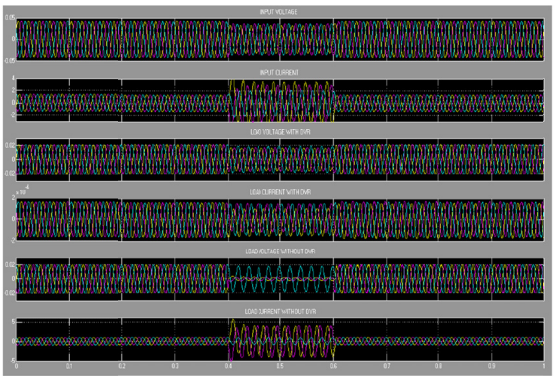

Fig. 20. Double line to ground fault

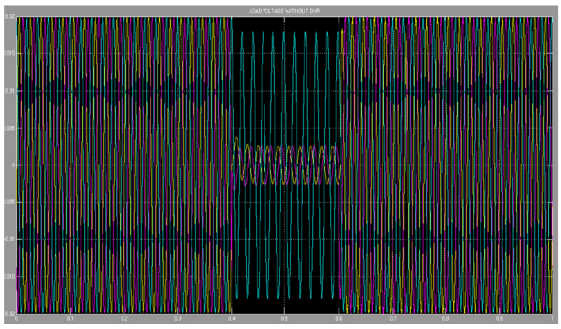

Fig. 21. Load voltage without DVR

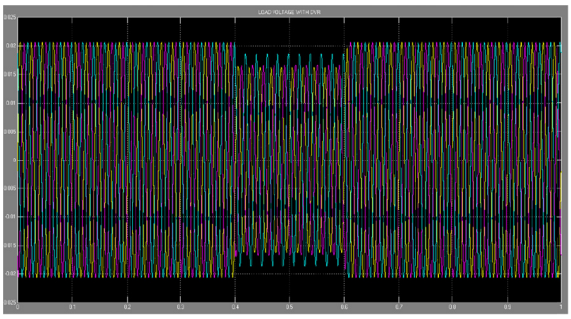

Fig. 22. Load voltage with DVR

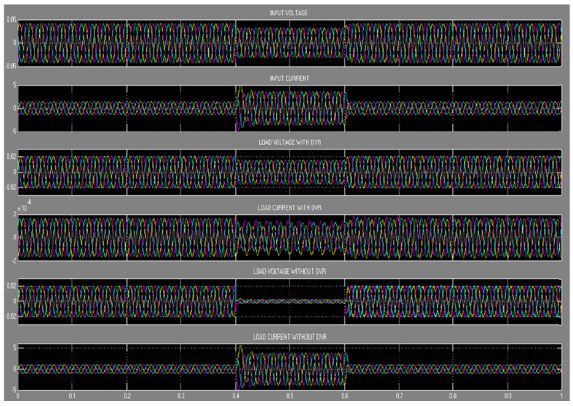

Fig. 23. Three phase to ground fault

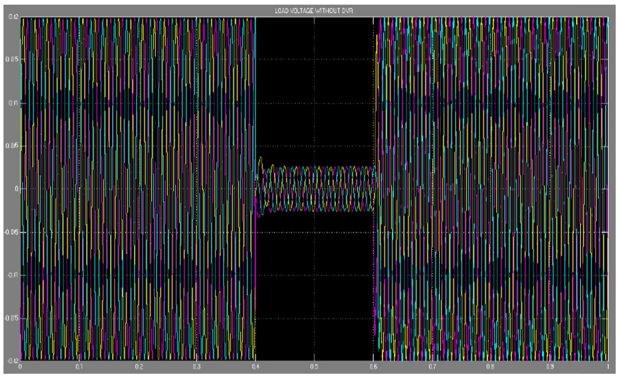

Fig. 24. Load voltage without DVR

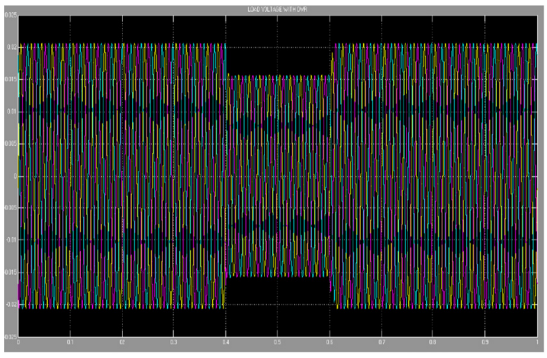

Fig. 25. Load voltage with DVR

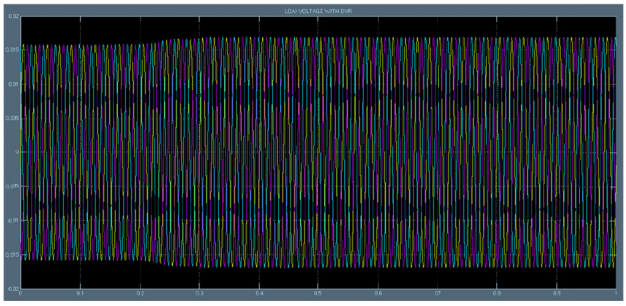

Fig. 26. Load voltage (single line to ground fault)

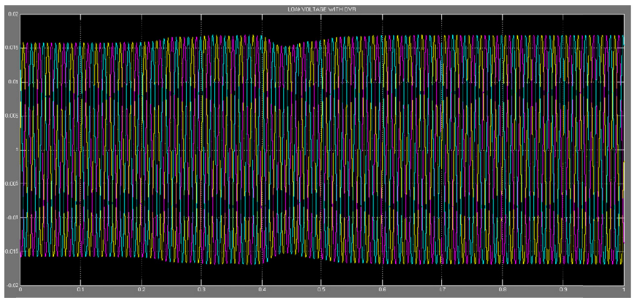

Fig. 27. Load voltage (Double line to ground fault)

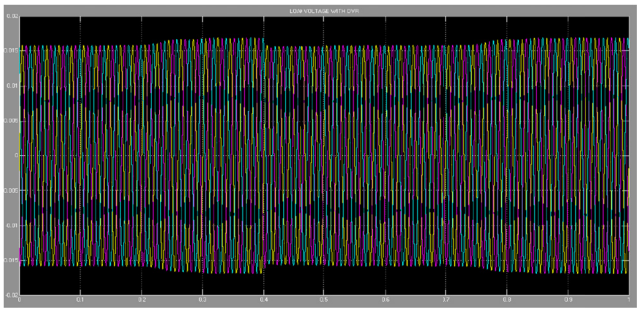

Fig. 28. Load voltage (three phase to ground fault)

TABLE VIII. COMPARISON OF THE TWO METHODS

	Phase	Conventional model (Figure 14)	Proposed model (Figure 15)
Distorted voltage	A	232	232
	B	234	234
	C	232	232
Injected voltage	A	158	183
	B	152	181
	C	137	183
Load voltage	A	390	415
	B	386	415
	C	369	415

VIII. CONCLUSION

The proposed DVR was tested for different fault conditions. From the obtained results, it can be concluded that the proposed DVR with MCFC and ultra capacitor is more efficient when compared to a conventional DVR design. However, it should be noted that conventional model took less simulation time to execute. The ode23s solver was selected even though it resulted to low speed since the odc15s solver proved even slower and the ode23t and ode23tb solvers gave convergence problem. Overall results show that the MCFC based DVR with fuzzy control could be an efficient solution for the improvement of power quality in the power system.

REFERENCES

[1] C. Sankaran, PowerQuality, CRC Press, 2001

[2] R. C. Dugan, S. Santoso, M. F. McGranaghan, H. W. Beaty, Electrical Power Systems Quality, McGraw Hill Professional, 2012

[3] T. Jimichi, H. Fujita, H. Akagi, "Design and experimentation of a dynamic voltage restorer capable of significantly reducing an energy-storage element", IEEE Transactions on Industry Applications, Vol.44, No.3, pp.817–825, 2008

[4] C. Gopinath, R. Ramesh, "Dynamic voltage restorer using ultra storage capacitor", International Conference on Sustainable Energy and Intelligent Systems, Chennai, India, pp.69–74, July 20-22, 2011

[5] J. Milewski, A. Miller, "Influences of the type and thickness of electrolyte on solid oxide fuel cell hybrid system performance", Journal of Fuel Cell Science and Technology, Vol. 3, No. 4, pp. 396-402, 2006

[6] D. Flynn, Modelling of power plant in Thermal Power Plant Simulation and Control, The Institution of Electrical Engineers, 2003

[7] J. Brouwer, F. Jabbari, E. M. Leal, T. Orr, "Analysis of a molten carbonate fuel cell: Numerical modeling and experimental validation", Journal of Power Sources, Vol. 158, No. 1, pp. 213-224, 2006

[8] S. Luri, I Etxeberria-Otadui, A. Rujas, E. Bilbao, A. Gonzalez, "Design of Supercapacitor based storage system for improved elevator application", IEEE Energy Conversion Congress and Exposition, Atlanta, USA, pp. 4534-4539, September 12-16, 2010

[9] J. G. Nielsen, F. Blaabjerg, N. Mohan, "Control strategies for dynamic voltage restorer compensating voltage sags with phase jump", 16th Annual IEEE Applied power electronics conference and exposition, Anaheim, USA, Vol. 2, pp. 1267-1273, March 4-8, 2001